Preparation and characterization of 0.5PMN-0.5PFN ceramics using [Fe$_{0.6}$, Mg$_{0.4}$]NbO$_4$ as precursor

N. S. ALMODÓVAR, R. FONT, J. PORTELLES
Facultad de Física-IMRE, Universidad de La Habana, Vedado, La Habana, 10400, Cuba;
Centro de Ciencias de la Materia Condensada, Universidad Nacional Autónoma de México,
Apartado Postal 2681, Ensenada, Baja California, México 22800

O. RAYMOND, E. MARTÍNEZ, J. M. SIQUEIROS
Centro de Ciencias de la Materia Condensada, Universidad Nacional Autónoma de México,
Apartado Postal 2681, Ensenada, Baja California, México 22800
E-mail: jesus@ccmc.unam.mx

A study of the calcination and sintering processes of 0.5PMN-0.5PFN ceramics prepared starting from the specifically designed precursor compound [Fe$_{0.6}$, Mg$_{0.4}$]NbO$_4$, is presented. The microstructural characteristics are determined using X-ray diffraction and scanning electron microscopy. The resulting dielectric properties of the PMN-PFN samples thus obtained were very good when compared with those reported in the literature, for samples prepared at higher calcination temperatures. The dielectric properties as functions of temperature and the hysteresis loops (P vs. E) under different external applied electric fields are reported. © *2003 Kluwer Academic Publishers*

1. Introduction
Considerable attention has been given to the studies of complex perovskites with general formula A(B′B″)O$_3$, such as Pb(Mg$_{1/3}$Nb$_{2/3}$)O$_3$, (PMN); Pb(Fe$_{1/2}$Nb$_{1/2}$)O$_3$, (PFN); Pb(Zn$_{1/3}$Nb$_{2/3}$)O$_3$, (PZN) and Pb(Fe$_{2/3}$W$_{1/3}$)O$_3$, (PFW) due, essentially, to their high dielectric permittivity, diffuse phase transition, electrostriction and induced piezoelectricity in their paraelectric phase [1–3]. Recently, Fe doped systems such as $(1 - x)$Pb(Mg$_{1/3}$Nb$_{2/3}$)O$_3$ + xPb(Fe$_{1/2}$Nb$_{1/2}$)O$_3$ (PMN-PFN) are being considered because of the possible coexistence of ferroelectricity and ferromagnetism and an interaction between those two phenomena [4, 5]. Applications of interest of these materials include devices such as multilayer capacitors, ferroelectric transformers, pyroelectric detectors, transducers, etc. [1–3]. In particular, PMN-PFN has very high permittivity values and polarization and by adding the coexistence of ferroelectricity and ferromagnetism to its properties the range of possible applications widens further [3, 4, 6].

Obtaining a pure phase of PMN-PFN is a difficult task because of the high volatility of lead. The solid solution reaction undergoes several heat treatments where lead may be lost rendering lead-deficient phases that usually include pyrochlores. It is well known that pyrochlores are highly detrimental to the dielectric properties of the ceramic [7]. It is the purpose of this investigation to obtain the 0.5PMN-0.5PFN compound by the traditional ceramic method, using a previously devel-oped precursor [8–12] which has already proven successful [10]. Dielectric characterization and hysteresis loop studies were performed in the resulting compound.

2. Experiment
MgO [Alfa (Johnson Matthey), 96%], Fe$_2$O$_3$ (Merck, 99%) and Nb$_2$O$_5$ [Alfa (Johnson Matthey), 99.5%] were used as starting reactants. The samples were prepared by the conventional ceramic method by mixing the starting powders with ethanol in an agate mortar for 4 hours at room temperature. The amount of each reagent for the preparation of the precursor compound was calculated according to the following equation

$$1/6\text{MgO} + 1/8\text{Fe}_2\text{O}_3 + 7/24\text{Nb}_2\text{O}_5$$
$$\rightarrow \text{Mg}_{1/6}\text{Nb}_{7/12}\text{Fe}_{1/4}\text{O}_2 \qquad (1)$$
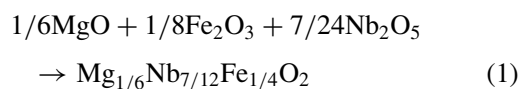
The oxide reagents were then sintered at 1200°C and as reported in [13] the resulting precursor was identified as [Fe$_{0.6}$, Mg$_{0.4}$]NbO$_4$, isostructural with the wolframite-like-FeNbO$_4$, where the Fe and Mg ions occupy the same crystal site. The difference in composition with respect to the hypothetical right hand member of Equation 1, would be due to non-reacted traces of niobium oxide which are assumed to be dispersed in the sample and its presence in the XRD analysis masked in the background of the diffraction data. A detailed structural and chemical study is in course and will be published elsewhere.

The obtained precursor was milled in an agate mortar with ethanol and mixed with PbO in the appropriate proportion, in correspondence to the stoichiometric amounts of Equation 1, according to the following equation:

$$Mg_{1/6}Nb_{7/12}Fe_{1/4}O_2 + PbO$$
$$\rightarrow 0.5Pb(Mg_{1/3}Nb_{2/3})O_3 + 0.5Pb(Fe_{1/2}Nb_{1/2})O_3 \qquad (2)$$
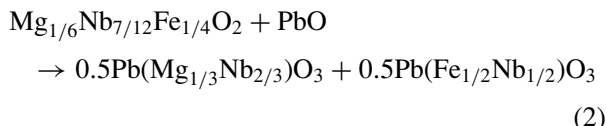
The resulting powders from the last mixing and milling were calcined at 850°C for 4 h to obtain the perovskite phase and uniaxially die-pressed into disks 10 mm in diameter and 1 mm thick at a pressure of 372 MPa. The samples were sintered at 1150°C for 15 min in a $PbZrO_3$ atmosphere. The calcined powders and sintered samples were studied by X-ray diffraction (XRD) in a Philips X'pert diffractometer with Cu ($\lambda_{k\alpha1} = 1,54056$ Å $\lambda_{k\alpha2} = 1,54439$ Å) anode. The permittivity and dielectric losses vs. temperature were measured with an HP 3238 RLC bridge in heating and cooling modes with a 1°C/min rate in both cases. The hysteresis loop at room temperature (20°C) was obtained in an RT-66 ferroelectric tester by Radiant Technologies Inc. coupled to a high voltage amplifier with maximum voltage of 4 kV. The microstructure of the samples was determined in a JSM 5300 scanning electron microscope (SEM) by JEOL.

3. Results and discussion
3.1. Calcination and sintering, XRD
Fig. 1 shows a diffractogram sequence of the powders calcined at different temperatures for 4 h. Fig. 1a corresponds to the powders calcined at 500°C and may be interpreted as a superposition of the patterns corresponding to the precursor phase $[Fe_{0.6}, Mg_{0.4}]NbO_4$
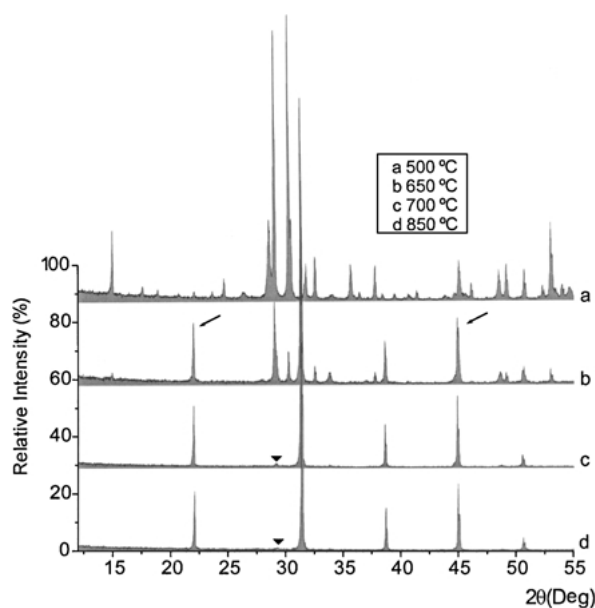
Figure 1 XRD spectra of 0.5PMN-0.5PFN samples calcined at different temperatures. Two peaks corresponding to the perovskite phase are signaled with arrows. The pyrochlore residual phase peaks are signaled with triangles.
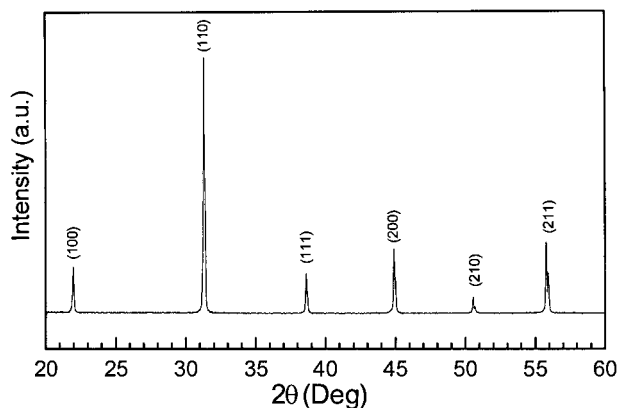
Figure 2 Diffractogram of a 0.5PMN-0.5PFN sample sintered at 1150°C showing a pure perovskite phase.

and that of PbO being the original components of the solid solution in the calcination process. In Fig. 1b, at 650°C, a conspicuous change in the relative intensity of the diffraction peaks at $2\theta = 22°$ and $40°$ (signaled with arrows in the figure) corresponding to the (100) and (200) planes, respectively, indicative of the appearance of the perovskite phase, is clearly observed, making evident the progress of the reaction towards the PMN-PFN formation.

The diffractogram corresponding to the powders calcined at 700°C shows the typical perovskite structure coexisting with a small quantity of a pyrochlore residual phase (labeled with a triangle in Fig. 1c, d) indicating that, around this temperature, the reaction between the precursor and the PbO to form the perovskite phase has nearly gone to completion. Heating above 700°C does not seem to produce significant changes in the resulting phase assamblage.

Finally, in Fig. 2, an XRD pattern corresponding to a pure, fully developed pyrochlore-free perovskite phase is shown for the samples sintered at 1150°C, demonstrating the effectiveness of the use of the $[Fe_{0.6}, Mg_{0.4}]NbO_4$ precursor in the preparation of the 0.5PMN-0.5PFN ceramics. Fig. 3 is an SEM micrograph of a sample sintered at 1150°C showing negligible porosity and well-crystallized, irregular shaped grains with a statistically determined mean grain size of 1.3 μm.

3.2. Dielectric analysis
Fig. 4 shows the dependence of the permittivity (ε) and dielectric loss ($\tan\delta$) on temperature at frequencies of 10 and 40 kHz. At these frequencies, the measured transition temperatures are 52°C and 51°C, respectively, with an experimental error of ±1°C, in close agreement with those reported by Sun-Gon Jun *et al.* [10]. It is also observed that the maxima of the permittivity and the dielectric loss curves do not coincide in temperature, a behavior characteristic of diffuse phase transitions. Actually, the tanδ maximum is not observed in the measured temperature range possibly due to a higher than expected conductive behavior of the material which manifests itself in a change of slope and an increase in dielectric losses starting at 50°C (see Fig. 4).
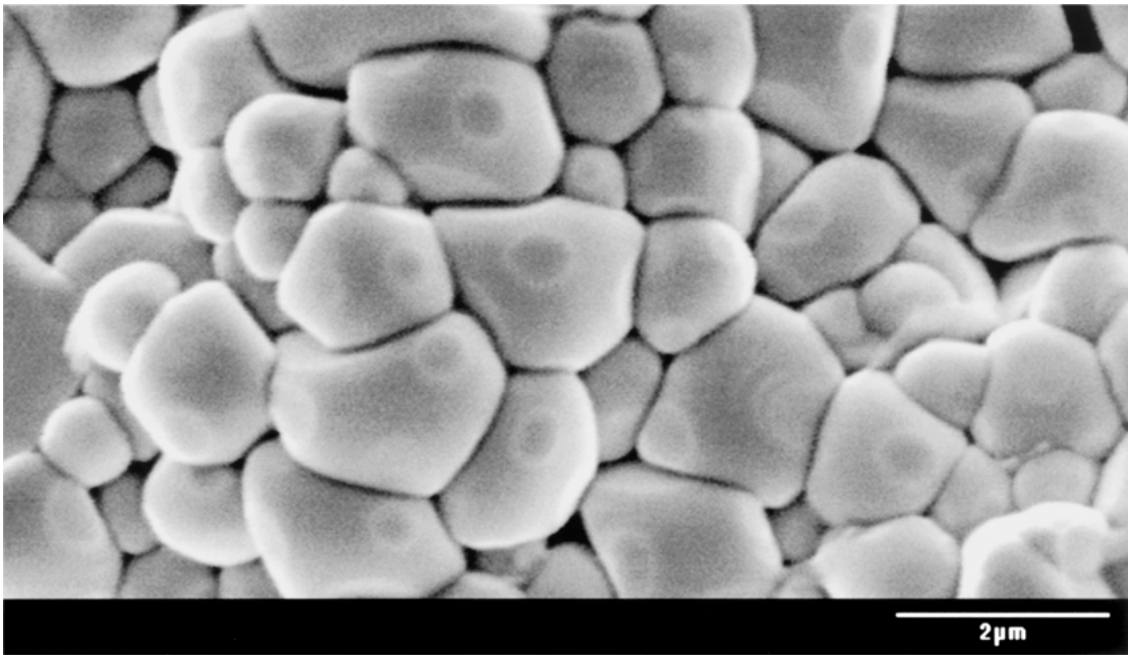
Figure 3 SEM micrograph of a 0.5PMN-0.5PFN sample sintered at 1150°C.
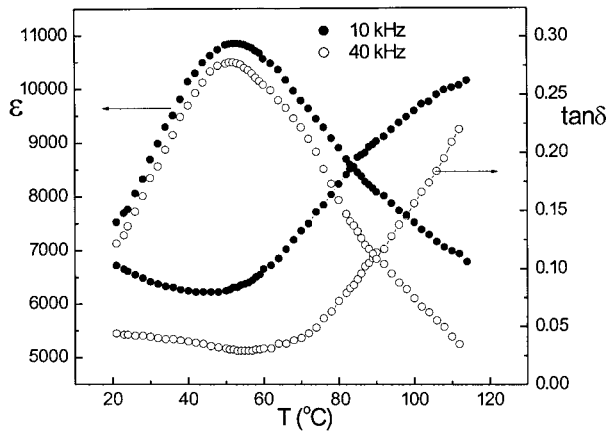
Figure 4 Permittivity and dielectric loss are plotted against temperature at two different frequencies for a 0.5PMN-0.5PFN sample sintered at 1150°C.

Figure 5 $\ln(1/\varepsilon_r - 1/\varepsilon_{r\,max})$ vs. $\ln(T - T_c)$ at 10 and 40 kHz of a 0.5PMN-0.5PFN sample sintered at 1150°C. In each case a numerical fit was performed to the experimental data to determine the slope γ and constant C.

To further analyze the observed behavior, use is made of the empirical expression of Pilgrim *et al.* [14]

$$\ln(1/\varepsilon_r - 1/\varepsilon_{r\,max}) = \ln C + \gamma \ln(T - T_c) \quad (3)$$

where ε_r is the relative dielectric permittivity at temperature T, $\varepsilon_{r\,max}$ is the maximum relative permittivity at the transition temperature and γ is a measure of the diffuseness of the transition. Using a numerical fitting program, a value of 1.8 for γ and -13 for lnC for measurements at 10 kHz were determined. At 40 kHz the values were $\gamma = 2.1$ and $\ln C = -17.9$ for the same sample. The process is illustrated in Fig. 5. These results suggest that the ceramic compound presents a diffuse phase transition, increasingly diffuse with increasing frequency, which is in good correspondence with the diffuse phase transitions theory (DPT) developed by Isupov-Smolenskii [15] and Cross [16]. This fact is explained by the enhancement of cationic disorder at the B sites of the ABO_3 perovskite structure which may be randomly occupied by Fe, Mg and Nb cations,

producing microregions with different local transition temperatures and as a result a wide transition curve in temperature. The presence of Fe^{2+} cations must also be considered with the consequent generation of O_2 vacancies in the structure and the influence they will have on the conductivity of the ceramic.

3.3. Ferroelectric hysteresis

Fig. 6 shows several hysteresis loops taken at different applied electric fields. The high dielectric energy associated to the enclosed area as well as high values of the remanent polarization (Pr) and coercive field (Ec) stand out in these measurements. The dependence of Pr with the electric field (E) is presented in Fig. 7 where a power series with the form $Pr = 4.7 \times 10^{-6} E + 1.1 \times 10^{-11} E^2$ was used to fit the experimental curve. It can be observed that saturation is not achieved at fields as high as 5 kV/cm. A linear behavior of the coercive field Ec

3087
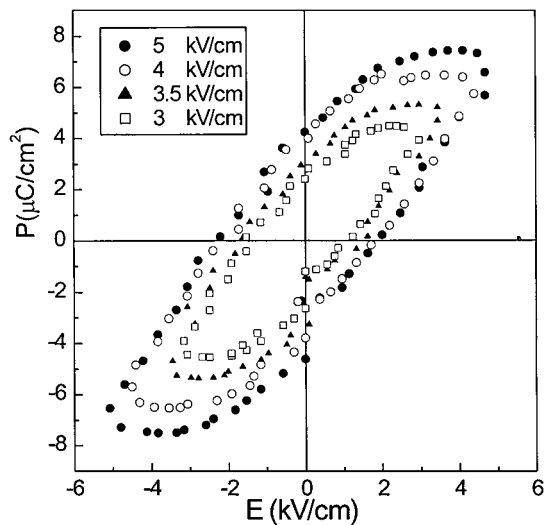
Figure 6 Hysteresis loops at different applied fields for a 0.5PMN-0.5PFN sample sintered at 1150°C.
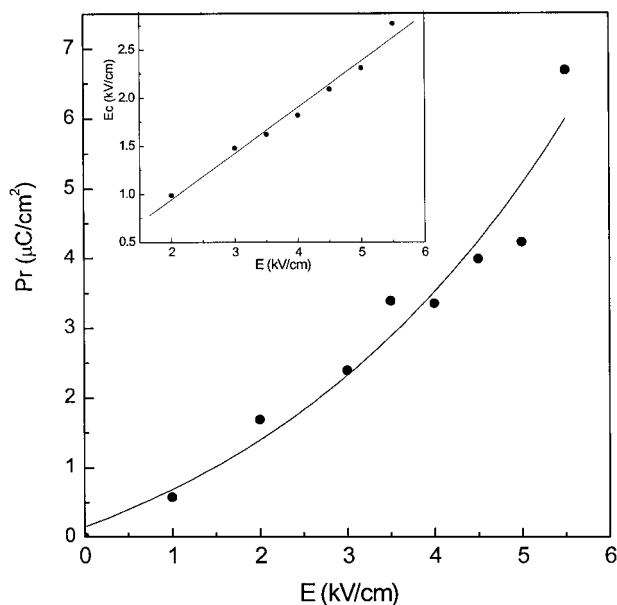
Figure 7 The remanent polarization (Pr) is plotted against electric field (E) for the 0.5PMN-0.5PFN sample sintered at 1150°C. Even at 5 kV/cm saturation is not reached. The inset shows the coercive electric field plotted against applied electric field.

was observed in the whole range of the applied electric field E as shown in the inset in Fig. 7.

4. Conclusions

The successful use of the $[Fe_{0.6}, Mg_{0.4}]NbO_4$ precursor in the synthesis of the pyrochlore-free 0.5PMN-0.5PFN ceramic at lower calcination temperatures than previously reported is presented. The resulting ceramics show high values for the dielectric permittivity, remanent polarization and coercive field. At a frequency of 10 kHz, the samples show a diffusive behavior that is accentuated as the frequency is increased up to 40 kHz. The values for the transition temperature agree with those reported by Sun-Gon Jun *et al.* [10]. The behavior of dielectric loss with temperature reflects the presence of conductive processes associated to the incorporation of the Fe^{2+} cation in the crystal structure.

References

1. Y. YAMASHITA, *Am. Ceram. Soc. Bull.* **73** (1994) 74.
2. R. E. WHATMORE, P. C. OSBOND and N. M. SHORROCKS, *Ferroelectrics* **76** (1987) 351.
3. T. R. SHROUT and A. HALLIYAL, *J. Amer. Ceram. Soc. Bull.* **66** (1987) 704.
4. X. S. GAO, X. Y. CHEN, J. YIN, J. WU and Z. G. LIU, *J. Mater. Sci.* **35** (2000) 5421.
5. A. S. IVANOV, R. TELLGREN, H. RUNDLOF, N. W. THOMAS and S. ANANTA, *J. Phys. Condens. Matter.* **12** (2000) 2393.
6. M. YOKOSUKA, *Jpn. J. Appl. Phys.* **32** (1993) 1142.
7. T. R. SHROUT and S. L. SWARTZ, *Mater. Res. Bull.* **189** (1983) 663.
8. S. M. GRUPTA and A. R. KULKARNI, *Mater. Chem. Phys.* **39** (1994) 98.
9. S. ANANTA and N. W. THOMAS, *J. Eur. Ceram. Soc.* **19** (1999) 2917.
10. S.-G. JUN, N.-K. KIM, J.-J. KIM and S.-H. CHO, *Mater. Lett.* **34** (1998) 336.
11. S. L. SWARTZ and T. R. SHROUT, *Mater. Res. Bull.* **17** (1982) 1245.
12. B. H. LEE, N. K. KIM, B. O. PARK and S. H. CHO, *Mater. Lett.* **33** (1997) 57.
13. N. S. ALMODOVAR, R. FONT, J. PORTELLES, O. RAYMOND and J. M. SIQUEIROS, *J. Mat. Sci.* **37** (2002) 5089.
14. S. M. PILGRIM, A. E. SUTHERLAND and S. R. WINZER, *J. Amer. Ceram. Soc.* **73** (1990) 3122.
15. G. A. SMOLENSKII, V. A. ISUPOV, A. I. AGRANOVSKAYA and S. N. POPOV, *Sov. Phys. Sol. State* **2**(11) (1961) 2584.
16. L. E. CROSS, *Ferroelectrics* **76** (1987) 241.